PHYSICAL REVIEW C VOLUME 45, NUMBER 3 MARCH 1992

Low-lying excitations in ^{176}Yb and ^{180}Hf from $(\vec{p},p')$ scattering at $E_p=98.4$ MeV

R. Perrino and R. De Leo
Universitá di Lecce and Sezione Istituto Nazionale di Fisica Nucleare di Lecce, I-73100 Lecce, Italy

A. D. Bacher, G. T. Emery,* C. W. Glover,† H. Nann, and C. Olmer
Indiana University Cyclotron Facility, Bloomington, Indiana 47405

R. V. F. Janssens
Argonne National Laboratory, Argonne, Illinois 60439

S. Y. van der Werf
Kernfysisch Versneller Instituut, NL-9747 AA Groningen, The Netherlands
(Received 2 May 1991)

The low-lying excited states of two rotational nuclei, ^{176}Yb and ^{180}Hf, have been investigated up to an excitation energy of 3.5 MeV by means of high-resolution inelastic scattering of 98.4-MeV polarized protons. The spins and excitation strengths of the observed levels have been deduced by comparing the measured cross sections and asymmetries with coupled-channel calculations. The deduced quadrupole, hexadecapole, and octupole strengths have been compared with the predictions of the interacting boson model in the *sdg*- and *sdf*-boson schemes.

PACS number(s): 25.40.Ep, 24.70.+s, 27.70.+q

I. INTRODUCTION

Recent experimental studies [1–7] have emphasized the role played by the quadrupole-octupole (QO) and the quadrupole-hexadecapole (QH) interactions in determining the $E3$ and $E4$ strength distributions among the low-lying states with $J^\pi=3^-$ and 4^+, respectively, in even-even collective nuclei with medium-heavy mass. In rotational nuclei the QO interaction is responsible for the splitting of the lowest octupole strength into four 3^- states belonging to rotational bands having K values from 0 to 3 (rotational character of the QO interaction). In vibrational nuclei, the same interaction splits up the quintuplet of two-phonon levels (one quadrupole, one octupole phonon) with spins ranging from 1^- to 5^-, which would be otherwise degenerate in energy at the sum of the excitation energies of the 2_1^+ and 3_1^- states, and would be excited only by two-step transitions through these levels (vibrational character of the QO interaction). In many nuclei, which do not correspond to the two limits just discussed, the low-lying octupole strength manifests itself in a more complex way. The experimental observations [1–3] are often intermediate between those described above. In spite of this complication, the interacting boson model (IBA), in the *sdf* expansion, seems to adequately reproduce the experimental distribution of low-lying octupole strength over a large range of nuclei. This has been shown by Pignanelli *et al.* [1] for medium-mass vibrational nuclei, and by Barfield *et al.* [2] for some rotational nuclei in the rare-earth region.

Up to now, the effect of the QH interaction on the distribution of the low-lying $0\hbar\omega$ hexadecapole strength in collective nuclei has not been fully understood because of the lack of systematic measurements. However, some experiments [3–7] on a few sample nuclei agree on the role played by the QH interaction in explaining the experimental strength of 4^+ levels located above the 4_1^+ state. In the vibrational nucleus ^{112}Cd the lowest 4_1^+ state is mainly excited [3] by a two-quadrupole-phonon component. The biggest hexadecapole strength resides at an excitation energy of 2.5 MeV, and is spread over a few 4^+ levels within an excitation energy interval of 1 MeV. A different situation has been found in some rotational nuclei such as ^{192}Os [4], ^{150}Nd [5], and ^{156}Gd [5,6], where the low-lying hexadecapole strength is dominated by the 4_1^+ state belonging to the ground-state (g.s.) rotational band, or as in ^{194,198}Pt [7] where the first three 4^+ states have nearly the same $E4$ strength. In Refs. [3–7] the QH interaction has been treated by coupling a *g* boson to the basic *sd* approximation of the IBA model (*sdg* expansion).

Recently, a clustering of 4^+ states has been found by Fujita *et al.* [8] in closed-shell nuclei with centroids between $16A^{-1/3}$ and $36A^{-1/3}$ MeV. These excitations exhaust from 3% to 11% of the energy-weighted sum rule (EWSR), and have a width of about 1 MeV; this clustering has been identified [8] with the low-energy hexadecapole resonance (LEHR).

In order to provide more information about the octupole, and especially of the hexadecapole, strength distributions in well-deformed heavy-mass nuclei, we have investigated in this work the low-lying states of ^{176}Yb and

*Present address: Bowdoin College, Brunswick, Maine 04011.
†Present address: Oak Ridge National Laboratory, Oak Ridge, Tennessee 37831.

^{180}Hf through a high-resolution inelastic proton scattering experiment.

II. EXPERIMENTAL PROCEDURE AND DATA REDUCTION

The experiments were performed at the Indiana University Cyclotron Facility with a polarized 98.4-MeV proton beam. Isotopically enriched (96.4% for ^{176}Yb, 93.9% for ^{180}Hf) targets of approximately 10 mg/cm^2 were used, and scattered protons were detected with the QDDM magnetic spectrograph. An example of final spectra is shown in Fig. 1 for ^{180}Hf. An overall energy resolution of about 50 keV was achieved. The strongest levels were all found below about 3.5 MeV. Excitation energies are reported in the first column of Table I. The asterisks in this column indicate some known levels, taken [9] from the Nuclear Data Sheets, and used for the energy calibration of the spectrograph focal plane detector. On average the energy values quoted in the present paper have an uncertainty of about 6 keV for the states below $E_x=1.5$ MeV for ^{176}Yb and $E_x=2.5$ MeV for ^{180}Hf, and a larger uncertainty, up to 20 keV, at higher energies, due to the lack of good reference levels.

Examples of measured cross sections and asymmetries are shown in Fig. 2 for ^{180}Hf. Those for ^{176}Yb are qualitatively similar. Coupled-channels (CC) calculations with the computer code ECIS [10] were performed to identify the multipolarity of the transitions and to determine their strengths. Data on the g.s. band were fitted in the framework of the symmetric rotational model. Optical model (OM) parameters were taken from the systematics of Nadasen *et al.* [11]. A search on the deformation parameters and on the real and imaginary OM potential depths was performed; a renormalization of the cross sections, due to uncertainties and inhomogenities of the target foils, was also considered. OM parameters are, in the usual notations, with depths in MeV and radii and diffusenesses in fm, and with the small changes performed in some potential depths: $V_0=32.27$, $r_0=1.217$, $a_0=0.693$, $W_v=9.77$, $W_s=0$, $r_w=1.419$, $a_w=0.547$, $V_{\mathrm{s.o.}}=4.95$, $W_{\mathrm{s.o.}}=-0.55$, $r_{\mathrm{s.o.}}=1.103$, $a_{\mathrm{s.o.}}=0.6$, $r_C=1.2$, for ^{176}Yb; $V_0=31.85$, $r_0=1.217$, $a_0=0.692$, $W_v=9.25$, $W_s=0$, $r_w=1.419$, $a_w=0.547$, $V_{\mathrm{s.o.}}=4.63$, $W_{\mathrm{s.o.}}=-0.51$, $r_{\mathrm{s.o.}}=1.105$, $a_{\mathrm{s.o.}}=0.6$, $r_C=1.2$ for ^{180}Hf. The CC predictions were found to agree within $\pm 12\%$ with the absolute values of cross sections normalized by target areal density, collected charges, and spectrograph solid angle. Equal deformation parameters were imposed to the different parts (real, imaginary, spin-orbit, and Coulomb) of the potential. As an example, the obtained fits for the 4_1^+ and 6_1^+ levels of ^{180}Hf are reported in Fig. 2. The deduced deformation values for the g.s. rotational bands are reported in the third column (first three lines) of Table I; in Table II the same values are compared with the results from Ref. [12], where the inelastic scattering of 65-MeV polarized protons was measured on many Er, Yb, Hf, and W isotopes.

The quadrupole deformation parameters found in this analysis are higher than those of Ref. [12]. The difference is around 7% and slightly outside the uncertainty of 6% derived from the normalization of our cross sections (uncertainty $\pm 12\%$); for ^{180}Hf the difference with analysis 1 of Ref. [12] is smaller and around 4%. Part of these

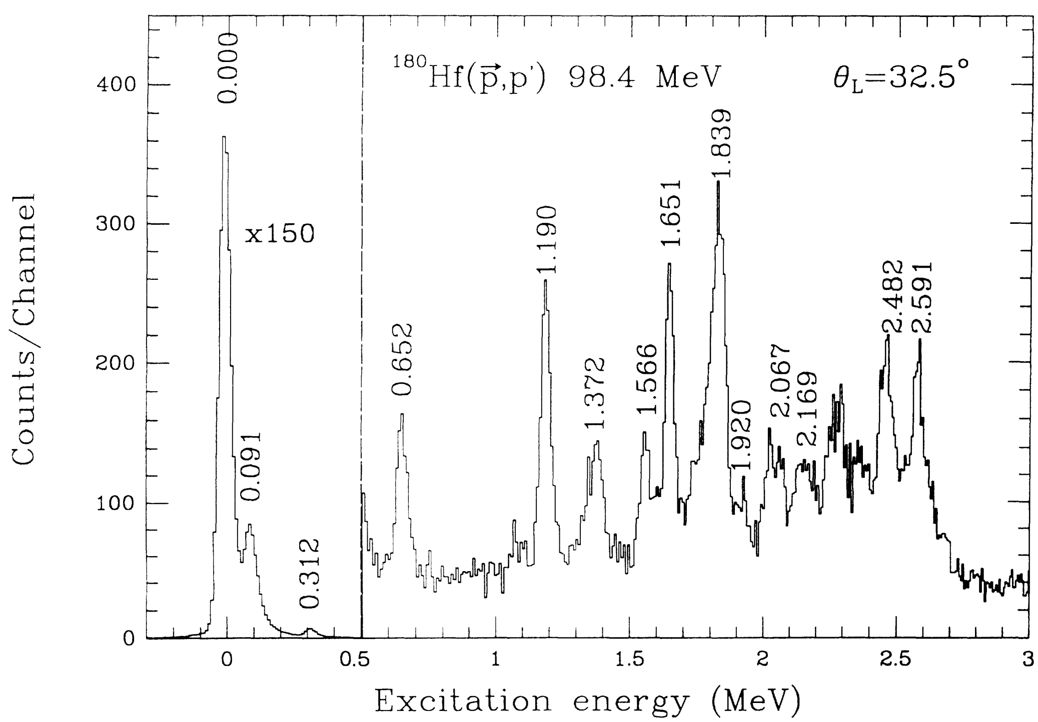

FIG. 1. ^{180}Hf($\vec{p}$,p') sample spectrum. Prominent states are indicated by the excitation energy (in MeV).

TABLE I. Excitation energies (E_x), spins (J^π), deformation parameters ($\beta_{p,p'}$), multipole moments [$M(E\lambda)_{p,p'}$] and energy-weighted sum-rule fractions (f_{EWSR}) for the excited states of ^{176}Yb and ^{180}Hf as derived from the analysis of the ($\vec{p},p'$) data.

E_x (MeV)	J^π	$\beta_{p,p'}$	$M(E\lambda)_{p,p'}$ ($e\,b^{\lambda/2}$)	f_{EWSR} (%)	Nucleus
0.081*	2^+	0.29*	2.62(16)	8.9	^{176}Yb
0.269*	4^+	−0.045[a]	0.018(25)	0.001	
0.567*	6^+	0.008[a]	−0.010(8)	0.001	
0.955	8^+				
1.261*	2^+	0.025	0.21(2)	0.92	
1.340	2^+	0.043	0.37(3)	2.88	
1.439*	4^+	0.023	0.12(1)	0.33	
1.542	3^-	0.024	0.16(1)	0.58	
1.622	3^-	0.041	0.27(2)	1.79	
1.715	5^-	0.015	0.06(1)	0.12	
1.855	b				
1.948	4^+	0.031	0.16(1)	0.81	
1.992	3^-	0.050	0.33(2)	3.27	
2.235	7^-				
2.303	2^+	0.030	0.25(2)	2.42	
2.462	4^+	0.028	0.15(1)	0.84	
2.528	3^-	0.042	0.28(2)	2.93	
2.721	b				
2.822	5^-	0.018	0.08(1)	0.28	
2.902	b				
3.033	4^+	0.024	0.12(1)	0.76	
3.088	3^-	0.030	0.20(2)	1.83	
3.187	4^+	0.022	0.11(1)	0.67	
3.324	4^+	0.022	0.11(1)	0.70	
0.091*	2^+	0.26[a]	2.41(15)	8.10	^{180}Hf
0.312*	4^+	−0.05[a]	−0.08(3)	0.032	
0.652*	6^+	0.004[a]	−0.041(6)	0.017	
1.086*	8^+				
1.190*	2^+	0.047	0.42(3)	3.17	
1.289*	2^+	0.019	0.18(2)	0.69	
1.372*	3^-	0.026	0.18(2)	0.63	
1.444	5^-	0.017	0.08(1)	0.13	
1.566*	4^+	0.022	0.12(1)	0.34	
1.651	3^-	0.038	0.26(2)	1.64	
1.715	5^-	0.014	0.06(1)	0.11	
1.740	3^-	0.019	0.13(1)	0.43	
1.804*	3^-	0.026	0.18(2)	0.83	
1.839	3^-	0.040	0.27(5)	2.00	
		−0.037[c]			
		−0.314[d]			
1.920	3^-	0.019	0.13(1)	0.47	
2.067	4^+	0.020	0.11(1)	0.37	
2.125	b				
2.169*	3^-	0.018	0.12(1)	0.48	
		−0.013[c]			
		−0.11[d]			

TABLE I. (*Continued*).

E_x (MeV)	J^π	$\beta_{p,p'}$	$M(E\lambda)_{p,p'}$ ($e\,b^{\lambda/2}$)	f_{EWSR} (%)	Nucleus
2.205	b				
2.257	4^+	0.018	0.10(1)	0.33	
2.295	b				
2.391	4^+	0.015	0.08(1)	0.24	
2.447*	5^-	0.027	0.12(1)	0.56	
2.482	3^-	0.029	0.20(2)	1.42	
2.533	3^-	0.018	0.12(1)	0.56	
2.591	4^+	0.022	0.12(1)	0.56	

[a]Values determined in the framework of the symmetric rotational model.
[b]Unknown spin.
[c]Two-step process through the 2_1^+ level used in CC calculation.
[d]Two-step process through the 3_1^- level used in CC calculation.
*Excitation energy taken from Ref. [8] and used for energy calibration.

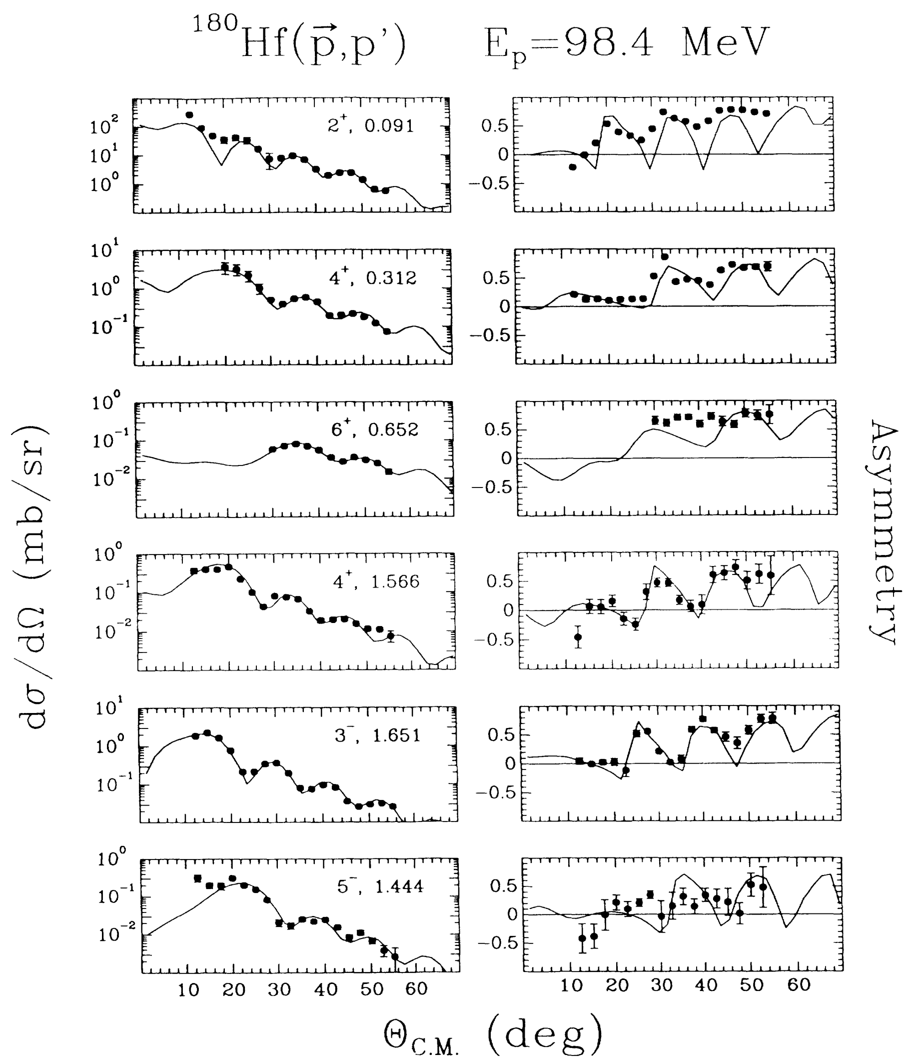

FIG. 2. Examples of differential cross sections (labeled by spin and excitation energy) and asymmetries observed in the ^{180}Hf($\vec{p}$,p') reaction at E_p=98.4 MeV. The solid curves are results of the CC calculations described in the text.

TABLE II. Comparison between the deformation parameters and multipole moments calculated in this paper and taken from Ref. [12], for the quoted levels of the g.s. rotational band.

E_x (MeV)	J^π	β_λ^R	β_λ^{wv}	β_λ^{ws}	β_λ^{ls}	β_λ^c	$M(E\lambda)^R_{pp'}$ ($e\,b^{\lambda/2}$)	$M(E\lambda)^I_{pp'}$ ($e\,b^{\lambda/2}$)	$M(E\lambda)^{ls}_{pp'}$ ($e\,b^{\lambda/2}$)	References	Nucleus
0.081	2^+	0.290	0.290	0.290	0.290	0.290	2.62(16)			This work	^{176}Yb
0.082	2^+	0.2714	0.2137	0.2985	0.3104	0.3133	2.436(32)	2.436(32)	2.436(32)	Ref. [12]	
0.269	4^+	−0.045	−0.045	−0.045	−0.045	−0.045	0.018(25)			This work	
0.272	4^+	−0.0478	−0.0333	−0.0588	−0.0604	−0.0538	−0.071(20)	−0.071(20)	−0.071(20)	Ref. [12]	
0.567	6^+	0.008	0.008	0.008	0.008	0.008	−0.0096(80)			This work	
0.565	6^+	−0.0090	−0.0062	−0.0168	−0.0141	−0.0063	−0.104(7)	−0.104(7)	−0.104(7)	Ref. [12]	
0.091	2^+	0.260	0.260	0.260	0.260	0.260	2.41(15)			This work	^{180}Hf
0.093	2^+	0.2431	0.3039	0.2366	0.2836	0.3001	2.260(24)	2.260(24)	2.260(24)	Ref. [12] (analysis 1)	
0.093	2^+	0.2507	0.1965	0.2514	0.2613	0.2754	2.304(35)	2.175(139)	2.098(107)	Ref. [12] (analysis 2)	
0.312	4^+	−0.050	−0.050	−0.050	−0.050	−0.050	−0.082(33)			This work	
0.309	4^+	−0.0567	−0.0792	−0.0558	−0.0738	−0.0843	−0.174(13)	−0.174(13)	−0.174(13)	Ref. [12] (analysis 1)	
0.309	4^+	−0.0562	−0.0983	0.0145	−0.0575	−0.0699	−0.170(14)	−0.455(98)	−0.059(36)	Ref. [12] (analysis 2)	
0.652	6^+	0.004	0.004	0.004	0.004	0.004	−0.041(6)			This work	
0.641	6^+	−0.0020	−0.0024	−0.0025	−0.0032	−0.0056				Ref. [12] (analysis 1)	
0.641	6^+	−0.0110	0.0812	−0.2159	0.0354	0.0479				Ref. [12] (analysis 2)	

discrepancies can be attributed to the different CC calculations performed in the present analysis and in Ref. [12]. For ^{176}Yb and for ^{180}Hf analysis 1, in Ref. [12], CC calculations were performed by imposing equal multipole moments to the different parts of the potential, while for ^{180}Hf analysis 2, different deformations (β_λ^i in Table II) were allowed [12] to the different potential parts. The hexadecapole parameters of the present analysis are instead lower than those of Ref. [12]. This is a consequence of the higher β_2 values which bring more strength in the 4_1^+ levels through two-step processes and second-order direct excitations; as a consequence direct first-order excitations are lowered.

Most of the remaining states were analyzed by using the direct excitation $0_{\text{g.s.}}^+ \to J^\pi$ scheme of CC calculations with Woods-Saxon first derivative (WSFD) form factors. A few cross sections and analyzing powers required two-step contributions via the 2_1^+ level for even-parity states, or via the 3_1^- level for odd-parity states. The asymmetry data have been useful in removing uncertainties in spin assignments and in the evaluation of multiple-excitation contributions. An example of obtained fits is reported in Fig. 2. Apart from the g.s. band, only 2^+, 3^-, 4^+, and 5^- states have been identified. The assigned spins and deformation parameters $\beta_{p,p'}$ are listed in the second and third columns of Table I. The $\beta_{p,p'}$ values have been converted, using the code BEL [13], into multipole moments $M(E\lambda)_{p,p'}$ and EWSR fractions (see the fourth and fifth columns of Table I). The $M(E\lambda)_{p,p'}$ for the g.s. rotational band levels have been obtained from the multipole expansion of the deformed optical potential (DOP):

$$M(E\lambda)_{p,p'} = \frac{Z \int V_{\text{DOP}}(r,\theta) Y_{\lambda 0}(\theta) r^{\lambda+2} dr\, d\Omega}{\int V_{\text{DOP}}(r,\theta) r^2 dr\, d\Omega} . \tag{2.1}$$

For the other levels the moments were derived from the usual collective WSFD transition potential:

$$M(E\lambda)_{p,p'} = \frac{Z\beta_\lambda \int V_{\text{WSFD}}(r) r^{\lambda+2} dr}{\int V_{\text{OM}}(r) r^2 dr} . \tag{2.2}$$

Only the real part of the V_{DOP}, V_{OM}, and V_{WSFD} potentials has been used in the evaluation of the multipole moments. The uncertainties quoted for the $M(E\lambda)_{p,p'}$ values in Tables I and II include contributions due to statistics, absolute normalizations, and, when present, to two-step or second-order processes. The last two are important for the quoted $M(E\lambda)$ uncertainties of the 4_1^+ and 6_1^+ levels. Within the quoted errors there is agreement in Table II between the quadrupole moments of the 2_1^+ levels deduced in the present analysis and in Ref. [12]. The agreement is worse for the hexadecapole moments of the 4_1^+ levels. These moments strongly depend upon the values of first- and second-order processes; these are nearly equal with opposite signs. Second-order contributions are instead dominant in the evaluation of the $M(E6)$ values.

The reduced transition probabilities

$$B(E\lambda)_{p,p'} = \frac{[M(E\lambda)_{p,p'}]^2}{2J_i+1} \tag{2.3}$$

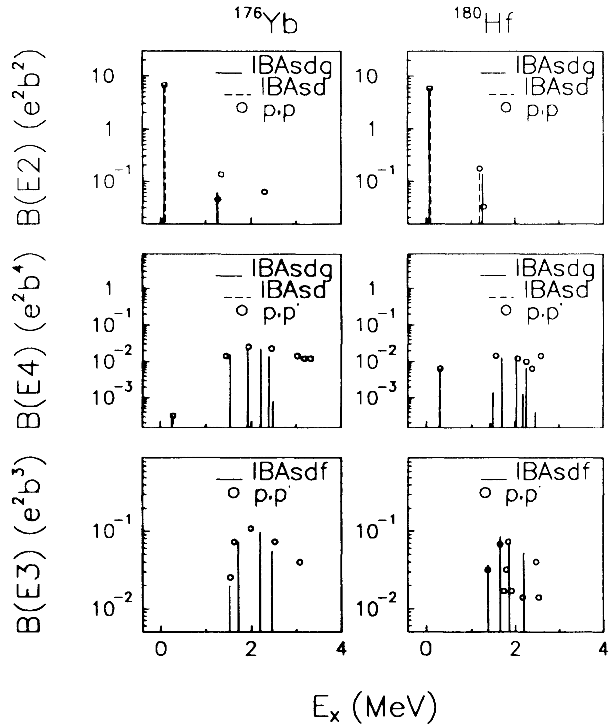

FIG. 3. Reduced transition probabilities (open points) for quadrupole (upper parts), hexadecapole (middle parts), and octupole (lower parts) excitations in ^{176}Yb and ^{180}Hf determined in the present experiment. Solid and dashed vertical lines are the results of the IBA calculations described in the text.

for the direct excitation from the g.s. of the $J^\pi = 2^+$, 4^+, and 3^- levels, are plotted in Fig. 3 versus the excitation energy. The three multipolarities have similar strength distributions in the two nuclei studied. In particular, the quadrupole strength (upper part of figure) is concentrated in the first 2_1^+ levels; this is the case even if the EWSR fraction is considered. This behavior is similar to that observed [3,14] for $E2$ excitations in other mass regions. The hexadecapole strength of the 4_1^+ levels (middle part of figure) is weak. The largest $E4$ strength is fragmented between 1.5 and 3.5 MeV, with major contributions in five or six levels. This behavior is different from that observed in all the other rotational nuclei investigated [4–7]. The octupole strength (bottom part of Fig. 3) shows no evidence of concentration in any single level. It has major contributions from about five levels, with a distribution pattern roughly consistent with the rotational character of the QO interaction.

Only $\sim 4\%$ and $\sim 2\%$ of the $E4$ EWSR has been found, respectively, in ^{176}Yb and ^{180}Hf up to an excitation energy of approximately $20A^{-1/3}$ MeV. These values are low to associate this strength with the LEHR reported in Ref. [8]. The same conclusions can be drawn concerning the octupole strength reported here and the low-energy octupole resonance [15] (LEOR).

III. IBA ANALYSES

In order to quantitatively evaluate the role played by the QO and QH interactions in ^{176}Yb and ^{180}Hf, we have compared IBA analyses [16] with the data. The version IBA-1, which does not distinguish neutron from proton bosons, has been used.

The multipole expansion of the *sd* Hamiltonian has been used:

$$H_{sd}=H_d+\mathrm{PAIR}+\mathrm{ELL}(D\cdot D)+\mathrm{QQ}(Q\cdot Q)+\mathrm{OCT}(O\cdot O)+\mathrm{HEX}(H\cdot H)\;. \quad (3.1)$$

A short version of this Hamiltonian (with $H_d=\mathrm{PAIR}=\mathrm{OCT}=\mathrm{HEX}=0$) has been found adequate in reproducing the excited levels of nuclei in the transitional region between the SU(3) (i.e., axially symmetric rotors) and O(6) (i.e., γ-unstable nuclei) limits [2,17]. The consistent Q formalism (CQF) of the IBA model is obtained if the same quadrupole (Q) and hexadecapole (H) operators are used both in the Hamiltonian and in the evaluation of the transition operators:

$$Q=(s^\dagger\tilde{d}+d^\dagger\tilde{s})^{(2)}+\mathrm{CHQ}(d^\dagger\tilde{d})^{(2)}\;, \quad (3.2)$$

$$H=(d^\dagger\tilde{d})^{(4)}\;. \quad (3.3)$$

The reduced transition probabilities then have the form: $B(E2)=(e_2Q)^2$; $B(E4)=(e_4H)^2$. The parameters of this Hamiltonian, listed in the *sd* columns of Table III, were obtained by fitting the lowest excitation energies and the $B(E2_1^+)$, $B(E2_2^+)$, and $B(E4_1^+)$ values. This Hamiltonian fails to reproduce the excitation energies and the strengths of 4^+ levels located higher than the 4_1^+ state (see the dashed vertical lines in Fig. 3). To account for this strength, it is necessary to consider the *sdg* expansion of the IBA model. In this expansion the Hamiltonian is formally the same of the *sd* one, with the only addition of the unperturbed g boson energy: $H_{sdg}=H_{sd}+H_g$. However, the transition operators suffer great changes since several additional modes now become available to form $L=2$ and 4 angular momenta:

$$Q=(s^\dagger\tilde{d}+d^\dagger\tilde{s})^{(2)}+\mathrm{Q2DD}(d^\dagger\tilde{d})^{(2)}+\mathrm{Q2DG}(g^\dagger\tilde{d}+d^\dagger\tilde{g})^{(2)}+\mathrm{Q2GG}(g^\dagger\tilde{g})^{(2)}\;, \quad (3.4)$$

$$H=(d^\dagger\tilde{d})^{(4)}+\mathrm{Q4GS}(g^\dagger\tilde{s}+s^\dagger\tilde{g})^{(4)}+\mathrm{Q4DG}(g^\dagger\tilde{d}+d^\dagger\tilde{g})^{(4)}\;. \quad (3.5)$$

With the hexadecapole terms (HEX or Q4Q4, see Table III) set to zero in H_{sd} and in H_{sdg}, only the parameters Q2DG and Q2GG are responsible for the QH interaction. They affect the excitation energy of higher 2^+ and 4^+ states and bring strength in the new terms of the H operator. Moreover, if sufficiently high in value, they also influence the quadrupole strength. The parameter Q2DG causes mixing between the pure *sd* and g configurations, while Q2GG produces splitting of the pure or degenerate g configurations.

The values derived from the fits for the Q2DG and Q2GG parameters (see Table III) suggest that, in both nuclei, the hexadecapole strength resulting from the in-

TABLE III. IBA parameters for the analyses described in the text. The codes [16] PHINT-FBEM have been used for the *sd* and *sdf* expansions, PHINTL-FBEML for the *sdg* one. The codes PHINT and PHINTL make use of different names and values for some parameters of identical meaning; these are QQ=Q2Q2*2, CHQ=Q2DD*$\sqrt{5}$, HEX=Q4Q4/5.

Parameter \ Analysis		Nucleus: ^{176}Yb			^{180}Hf		
		sd	*sdg*	*sdf*	*sd*	*sdg*	*sdf*
H_d	(MeV)	0.0	0.0	0.0	0.0	0.0	0.0
PAIR	(MeV)	0.0	0.0	0.0	0.0	0.0	0.0
ELL	(MeV)	0.012	0.012	0.012	0.009	0.009	0.009
QQ	(MeV)	−0.04		−0.04	−0.06		−0.06
Q2Q2	(MeV)		−0.02			−0.03	
OCT	(MeV)	0.0	0.0	0.0	0.0	0.0	0.0
HEX	(MeV)	0.0		0.0	0.0		0.0
Q4Q4	(MeV)		0.0			0.0	
H_g	(MeV)		0.80			0.60	
H_f	(MeV)			0.87			0.54
FELL	(MeV)			0.028			0.037
FQQ	(MeV)			0.009			0.008
FEX	(MeV)			0.019			0.040
CHQ		−1.7		−1.7	−1.1		−1.1
Q2DD			−0.76			−0.54	
Q2DG			0.05			0.26	
Q2GG			−1.14			−0.64	
Q4GS			17.5			3.4	
Q4DG			15.0			1.4	
e_2	(e b)	0.127	0.127	0.127	0.142	0.140	0.142
e_4	(e b^2)	0.007	0.006	0.007	0.037	0.023	0.037
e_3	(e b$^{3/2}$)			0.07			0.07
e_{3df}	(e b$^{3/2}$)			−0.09			−0.01

troduction of the g-boson configuration is more split than mixed with the sd one. Moreover, the obtained Q2DG and Q2GG values are higher than those required [3] for ^{112}Cd, revealing the different character and the importance of the QH interaction in the rotational nuclei ^{176}Yb and ^{180}Hf.

The sdf expansion of the IBA model has been used to reproduce the octupole strength. The Hamiltonian is written as $H_{sdf}=H_{sd}+H_f+H_{df}$, where H_f is the unperturbed f-boson energy, and H_{df} is the part of the Hamiltonian responsible for the QO interaction. The expansion of H_{df} into a dipole, quadrupole, and an octupole term is given as

$$H_{df}=\mathrm{FELL}(L_d\cdot L_f)+\mathrm{FQQ}(Q_d\cdot Q_f) -5\,\mathrm{FEX}[(d^\dagger \tilde{f})^{(3)}(f^\dagger \tilde{d})^{(3)}]^{(0)}\ . \quad (3.6)$$

This Hamiltonian has been used successfully both in the $A\sim100$ (Ref. [1]) and $A\sim150$–180 (Ref. [2]) regions, and has been retained here. The meaning of the three terms has been extensively discussed in Refs. [1] and [2]. All three terms of H_{df} are able to break the energy degeneracy of the two-phonon quintuplet $(1^-,2^-,3^-,4^-,5^-)$, each producing a different spin sequence, but only the quadrupole term FQQ changes the sd configuration, thus transferring part of the octupole strength from the 3_1^- level to higher-lying 3^- states. The following simplified parametrization, without second-order terms, has been assumed to evaluate the octupole reduced transition probabilities:

$$B(E3)=[e_3(s^\dagger\tilde{f}+f^\dagger\tilde{s})^{(3)}+e_{3df}(d^\dagger\tilde{f}+f^\dagger\tilde{d})^{(3)}]^2\ . \quad (3.7)$$

The results of a search for the best sdf parameters, performed by fitting the available 3^- level excitation energies and reduced transition probabilities, are presented in Table III (sdf column) and in the lower parts of Fig. 3 with the vertical full lines. The deduced parameters agree within 80 keV with the systematics of Ref. [2] performed on other nuclei in the same mass region. The agreement is noteworthy considering that the emphasis in the present analysis has been put on the reproduction of the $B(E3)$ strength distribution, while in Ref. [2] the reproduction of the level sequence of the different (K^π) octupole bands was emphasized. The last information is not yet available in the nuclei here explored.

IV. CONCLUSIONS

The low-lying quadrupole, hexadecapole, and octupole strengths in ^{176}Yb and ^{180}Hf have been measured through an high-resolution inelastic scattering of 98.4-MeV polarized protons. Similar distributions for the different strengths in the two nuclei have been found. As in other nuclear mass regions, the quadrupole strength is concentrated in the 2_1^+ levels. A weak hexadecapole strength resides in the 4_1^+ states, but a considerable amount lies equifragmented in six or seven 4^+ levels located between 1.5 and 3.5 MeV. To reproduce this behavior, the sdg version of the IBA model is necessary, and a QH interaction stronger than that of the vibrational nucleus ^{112}Cd, and with a different character, is required. The octupole strength is strongly influenced by the QO interaction and it lies nearly equifragmented into four or five 3^- levels; this is evidence for the rotational character of the QO interaction in these nuclei.

ACKNOWLEDGMENTS

We would like to thank W. Jones and D. Miller for their help in the first part of the experiment. This work was supported in part by the "Stichting voor Fundamenteel Onderzoek der Materie" (FOM) with financial support from the "Nederlandse Organisatie voor Wetenschappelijk Onderzoek" (NWO) and by the U. S. National Science Foundation.

[1] M. Pignanelli, N. Blasi, S. Micheletti, R. De Leo, M. A. Hofstee, J. M. Schippers, S. Y. van der Werf, and M. N. Harakeh, Nucl. Phys. **A519**, 567 (1990).
[2] A. F. Barfield, B. R. Barrett, J. L. Wood, and O. Scholten, Ann. Phys. (N.Y.) **182**, 344 (1988).
[3] R. De Leo, N. Blasi, S. Micheletti, M. Pignanelli, W. T. A. Borghols, J. M. Schippers, S. Y. van der Werf, G. Maino, and M. N. Harakeh, Nucl. Phys. **A504**, 109 (1989).
[4] F. Todd Baker, A. Sethi, V. Penumetcha, G. T. Emery, W. P. Jones, M. A. Grimm, and M. L. Whiten, Phys. Rev. C **32**, 2212 (1985); Nucl. Phys. **A501**, 546 (1989).
[5] H. C. Wu, A. E. L. Dieperink, O. Scholten, M. N. Harakeh, R. De Leo, M. Pignanelli, and I. Morrison, Phys. Rev. C **38**, 1638 (1988).
[6] P. B. Goldhorn, M. N. Harakeh, Y. Iwasaki, L. W. Put, and F. Zwarts, Phys. Lett. **103B**, 291 (1981).
[7] A. Sethi, F. Todd Baker, G. T. Emery, W. P. Jones, and M. A. Grimm, Jr., Nucl. Phys. **A518**, 536 (1990).
[8] Y. Fujita, M. Fujiwara, S. Morinobu, I. Katayama, T. Yamazaki, T. Itahashi, H. Ikegami, and S. I. Hayakawa, Phys. Rev. C **40**, 1595 (1989).
[9] E. Brown, Nucl. Data Sheets **52**, 150 (1987); D. J. Horen and B. Harmatz, *ibid.* **19**, 405 (1976).
[10] J. Raynal, computer code ECIS (private communication).
[11] A. Nadasen, P. Schwandt, P. P. Singh, W. W. Jacobs, A. D. Bacher, P. T. Debevec, M. D. Kaitchuck, and J. T. Meek, Phys. Rev. C **23**, 1023 (1981).
[12] T. Ichihara, H. Sakaguchi, N. Nakamura, T. Noro, F. Ohtani, H. Sakamoto, H. Ogawa, M. Yosoi, M. Ieiri, N. Isshiki, and S. Kobayashi, Phys. Rev. C **29**, 1228 (1984); H. Ogawa, H. Sakaguchi, M. Nakamura, T. Noro, H. Sakamoto, T. Ichihara, M. Yosoi, M. Ieiri, N. Isshiki, Y. Takeuchi, and S. Kobayashi, *ibid.* **33**, 834 (1986).
[13] M. N. Harakeh, BEL Report No. KVI-77, KVI Groningen, 1981 (unpublished).
[14] M. Pignanelli, S. Micheletti, N. Blasi, R. De Leo, W. T. A. Borghols, J. M. Schippers, S. Y. van der Werf, and M. N. Harakeh, Phys. Lett. B **202**, 470 (1988); R. De Leo, L. Lagamba, N. Blasi, S. Micheletti, M. Pignanelli, M. Fujiwara, K. Hosono, I. Katayama, N. Matsuoka, S. Morinobu, T. Noro, S. Matsuki, H. Okamura, J. M. Schippers, S. Y. van der Werf, and M. N. Harakeh, *ibid.*

226, 5 (1989).
[15] A. Higashi, K. Katori, M. Fujiwara, H. Ikegami, I. Katayama, S. Morinobu, M. Tosaki, S. I. Hayakawa, N. Ikeda, and H. Miyatake, Phys. Rev. C **39**, 1286 (1989); J. M. Moss *et al., ibid.* **18**, 741 (1978).
[16] O. Scholten, computer program package PHINT (private communication).
[17] R. F. Casten, W. Frank, and P. von Brentano, Nucl. Phys. **A444**, 133 (1985).